Elsevier Editorial System(tm) for Carbohydrate Polymers
Manuscript Draft

Manuscript Number: CARBPOL-D-15-01029R1

Title: The nanostructural characterization of strawberry pectins in pectate lyase or polygalacturonase silenced fruits elucidates their role in softening

Article Type: Research Paper

Keywords: Atomic force microscopy; cell wall; Fragaria × ananassa; fruit softening; homogalacturonan; pectins

Corresponding Author: Dr. Jose A. Mercado,

Corresponding Author's Institution: Universidad de Malaga

First Author: Sara Pose

Order of Authors: Sara Pose; Andrew R Kirby; Candelas Paniagua; Keith W Waldron; Victor J Morris; Miguel A Quesada; Jose A. Mercado

Abstract: To ascertain the role of pectin disassembly in fruit softening, chelated- (CSP) and sodium carbonate-soluble (SSP) pectins from plants with a pectate lyase, FaplC, or a polygalacturonase, FaPG1, downregulated by antisense transformation were characterized at the nanostructural level. Fruits from transgenic plants were firmer than the control, although FaPG1 suppression had a greater effect on firmness. Size exclusion chromatography showed that the average molecular masses of both transgenic pectins were higher than that of the control. Atomic force microscopy analysis of pectins confirmed the higher degree of polymerization as result of pectinase silencing. The mean length values for CSP chains increased from 84 nm in the control to 95.5 and 101 nm, in antisense FaplC and antisense FaPG1 samples, respectively. Similarly, SSP polyuronides were longer in transgenic fruits (61, 67.5 and 71 nm, in the control, antisense FaplC and antisense FaPG1 samples, respectively). Transgenic pectins showed a more complex structure, with a higher percentage of branched chains than the control, especially in the case of FaPG1 silenced fruits. Supramolecular pectin aggregates, supposedly formed by homogalacturonan and rhamnogalacturonan I, were more frequently observed in antisense FaPG1 samples. The larger modifications in the nanostructure of pectins in FaPG1 silenced fruits when compared with antisense pectate lyase plants correlate with the higher impact of polygalacturonase silencing on reducing strawberry fruit softening.

The nanostructural characterization of strawberry pectins in pectate lyase or polygalacturonase silenced fruits elucidates their role in softening

Sara Posé[a1], Andrew R. Kirby[b], Candelas Paniagua[a], Keith W. Waldron[b], Victor J. Morris[b], Miguel A. Quesada[c], José A. Mercado[a]

[a]Instituto de Hortofruticultura Subtropical y Mediterránea "La Mayora" (IHSM-UMA-CSIC), Departamento de Biología Vegetal, Universidad de Málaga, 29071, Málaga, Spain

[b]Institute of Food Research, Norwich Research Park, Colney, Norwich, NR4 7UA, UK

[c]Departamento de Biología Vegetal, Universidad de Málaga, 29071, Málaga, Spain

Author's emails:

Sara Posé: S.Pose@leeds.ac.uk; Andrew R. Kirby: andrewkirby1966@gmail.com; Candelas Paniagua: candelaspc@uma.es; Keith W. Waldron: keith.waldron@ifr.ac.uk; Victor J. Morris: vic.morris@ifr.ac.uk; Miguel A. Quesada: quefe@uma.es; José A. Mercado: mercado@uma.es

*Corresponding author:

José A. Mercado

Instituto de Horticultura Subtropical y Mediterránea "La Mayora", IHSM-UMA-CSIC, Departamento de Biología Vegetal, Universidad de Málaga, Campus Teatinos s/n, 29071, Málaga, Spain

e-mail: mercado@uma.es; Fax: +34 952 13 20 00

[1]Present address: Centre for Plant Sciences, Faculty of Biological Sciences, University of Leeds, Leeds, LS2 9JT, UK

Abstract

To ascertain the role of pectin disassembly in fruit softening, chelated- (CSP) and sodium carbonate-soluble (SSP) pectins from plants with a pectate lyase, *FaplC*, or a polygalacturonase, *FaPG1*, downregulated by antisense transformation were characterized at the nanostructural level. Fruits from transgenic plants were firmer than the control, although *FaPG1* suppression had a greater effect on firmness. ~~Gel filtration~~ Size exclusion chromatography showed that the average molecular masses of both transgenic pectins were higher than that of the control. Atomic force microscopy analysis of pectins confirmed the higher degree of polymerization as result of pectinase silencing. The mean length values for CSP chains increased from 84 nm in the control to 95.5 and 101 nm, in antisense *FaplC* and antisense *FaPG1* samples, respectively. Similarly, SSP polyuronides were longer in transgenic fruits (61, 67.5 and 71 nm, in the control, antisense *FaplC* and antisense *FaPG1* samples, respectively). Transgenic pectins showed a more complex structure, with a higher percentage of branched chains than the control, especially in the case of *FaPG1* silenced fruits. Supramolecular pectin aggregates, supposedly formed by homogalacturonan and rhamnogalacturonan I, were more frequently observed in antisense *FaPG1* samples. The larger modifications in the nanostructure of pectins in *FaPG1* silenced fruits when compared with antisense pectate lyase plants correlate with the higher impact of polygalacturonase silencing on reducing strawberry fruit softening.

Keywords: Atomic force microscopy, cell wall, *Fragaria* × *ananassa*, fruit softening, homogalacturonan, pectins

Chemical compounds studied in this article

Galacturonan (PubChem CID: 445929)

Abbreviations: AFM, atomic force microscopy; APEL, antisense pectate lyase plants; APG, antisense polygalacturonase plants; CDTA, cyclohexane-trans-l,2-diamine tetraacetate; CSP, chelated soluble pectins; FTIR, Fourier transform infrared spectroscopy; HGA, homogalacturonan; LN, number-average contour length; LW, weight-average contour length; PDI, polydispersity index; PG,

polygalacturonase; PL, pectate lyase; RGI, rhamnogalacturonan I; SEC, size exclusion chromatography; SSP, sodium carbonate soluble pectins

1. Introduction

Strawberry (*Fragaria* × *ananassa* Duch.) is the most economically important edible soft fruit, which is characterized by its delicious flavour, intense colour, soft texture and high nutritional value. Besides its economic importance, several authors have proposed strawberry as a model for the study of the ripening process in non-climacteric fruits (Posé et al., 2011). The fast softening of this fruit determines its short post harvest life, which results in large loses due to over-softening, bruising and subsequent fungal infections that generally are associated with this process.

It is generally accepted that textural changes during ripening of fleshy fruits, mainly a decrease in firmness, are caused by a reduction of cell to cell interaction due to the dissolution of the middle lamella, a loosening of the primary cell wall and a reduction in cell turgor (Goulao & Oliveira, 2008; Mercado, Pliego-Alfaro, & Quesada, 2011). However, this last process is less well studied and is difficult to separate from the previously mentioned changes in cell wall structure. Amongst the different components that form the cell wall, polyuronides are the polymers most likely to be extensively modified during ripening. This involves pectin solubilization, i.e. an increase in the content of polyuronides loosely bound to the wall, and depolymerization and the loss of neutral sugars from pectin side-chains (Brummell, 2006; Goulao & Oliveira, 2008; Paniagua et al., 2014). These changes are due to the coordinated action of cell wall modifying enzymes, such as polygalacturonase (PG), pectate lyase (PL), pectin methyl esterase, β-galactosidase or α-arabinofuranosidase, which are generally encoded by ripening-related genes (Brummell & Harpster, 2001; Goulao & Oliveira, 2008; Mercado et al., 2011). Amongst these enzymes PG (EC 3.2.1.15) has been the most studied because certain fruits, e.g. tomato, peach or avocado, possess relatively high levels of PG activity, which correlate with the rate of the softening process (Brummell & Harpster, 2001). PG was also the first hydrolase to be examined using transgenic methods in tomato (Sheehy, Kramer, & Hiatt, 1988; Smith et al., 1988). However, the minor effect of PG silencing on tomato softening led to the

view that PG-mediated pectin disassembly during ripening makes only a small contribution to fruit softening (Hadfield & Bennett, 1998; Brummell & Harpster, 2001). More recent studies on strawberry, apple and papaya have challenged this hypothesis, suggesting a key role for pectin modifications in fruit softening (Jiménez-Bermúdez et al., 2002; Quesada et al., 2009; Youssef et al., 2009; Atkinson et al., 2012; Youssef et al., 2013; Fabi et al., 2014). ~~Thus, the down-regulation of a PL (EC 4.2.2.2) or a PG gene in strawberry significantly reduced fruit softening (Jiménez-Bermúdez et al., 2002; Quesada et al., 2009; Youssef et al., 2009; Youssef et al., 2013). Similarly, silencing of the PG1 gene in apple, a crisp fruit with completely different textural features to strawberry, also reduced softening (Atkinson et al., 2012). In papaya, the transient expression of *cpPG1* induced pulp softening, suggesting its central role in the ripening of this fruit (Fabi et al., 2014).~~

~~Compared with tomato, PG enzymatic activity is low in strawberry during ripening, and PL activity has still not been detected (Jiménez-Bermúdez et al., 2002; Villarreal, Rosli, Martínez, & Civello, 2008; Posé et al., 2011). However,~~ Ripening-specific genes encoding ~~both kinds~~ PG or PL (EC 4.2.2.2) enzymes have been described in strawberry (Medina-Escobar, Cárdenas, Moyano, Caballero, & Muñoz-Blanco, 1997; Villarreal, Rosli, Martínez, & Civello, 2008; Quesada et al., 2009) and their roles in fruit softening evaluated by means of a functional approach. In previous studies, our research group obtained transgenic strawberry plants expressing antisense sequences of the *FaplC* gene, encoding a PL (Jiménez-Bermúdez, et al. 2002; APEL lines) or the *FaPG1* gene, encoding a PG (Quesada et al., 2009; APG lines). Ripe fruits from both transgenic genotypes were significantly firmer than the wild type fruits. Based on their sequences, both genes encode putative endo-pectinases with a common target, de-esterified homogalacturonans (HGA), a major component of the primary cell wall and middle lamella. However, the mechanisms of action of PL and PG are different as are their optimum pH for enzymatic activity. Thus, PL cleaves HGA by β-elimination in the presence of divalent cations with an *in vitro* optimal pH ~ 8 (Marín-Rodríguez, Orchard, & Seymour, 2002). The PG degrades HGA by hydrolysis at acidic pH from 3.3 to 6.2 (Sénéchal, Wattier, Rustérucci, & Pelloux, 2014). Chemical analysis of cell wall extracts from APEL and APG transgenic

fruits revealed that the silencing of both pectinases reduced middle lamella dissolution and pectin solubilization~~, as evidenced by the amount of ionically and covalently bound pectins being found to be higher in the transgenic cell walls than in wild-type~~ (Santiago-Doménech et al., 2008; Posé et al., 2013). Additionally, ~~gel filtration~~ size exclusion chromatography results revealed higher molecular masses for the polymers present in the pectin fractions from the transgenic samples, which is consistent with a decreased depolymerization of these polyuronides.

In general, cell wall hydrolases involved in fruit softening are encoded by large gene families, within which a high degree of functional redundancy has been observed (Vicente, Saladié, Rose, & Labavitch, 2007; Goulao & Oliveira, 2008). ~~This is one of the main points put forward to explain the limited success obtained in most research projects aimed at reducing fruit softening by down-regulating a specific cell wall gene. However,~~ It is unclear why a fruit invests energy on the simultaneous expression of PG and PL enzymes acting on the same pectin domain, both having a key role on strawberry softening. The enzymatic differences between PG and PL are not enough to explain this redundancy. If these enzymes act on different targets within the pectin matrix, the pectic chains of these two differently silenced transgenic lines might show different degrees of polymerization and branching. This type of structural modification can be characterized by atomic force microscopy (AFM) at the nano-structural level~~. AFM allows the characterisation of individual pectin chains within a sample with minimal sample preparation~~ (Morris, Kirby, & Gunning, 2010). This technique has only recently been used to investigate pectin disassembly processes during fruit ripening (Paniagua et al., 2014). The main goal of this research was to analyze at the nano-structural level pectins from APG and APEL transgenic fruits to reveal the different effect of each enzyme in the pectin matrix and its implications on the mechanical properties of cell walls. Additional information has been obtained through the use of Fourier transform infrared spectroscopy (FT-IR) and size exclusion chromatography analysis (SEC). Based on previous studies, the present research has focused the nanostructural characterization of pectins which are ionically and covalently bound within the cell wall, since these fractions showed the most extensive changes as a result of *FaPG1* or *FaplC* genes silencing (Santiago-Doménech et al., 2008; Posé et al., 2013).

2. Material and methods

2.1. Plant material

Control, non-transformed, strawberry plants (*Fragaria* × *ananassa*, Duch., cv. 'Chandler'), transgenic antisense *FaplC* plants (line APEL39, described in Jiménez-Bermúdez et al. (2002) and Santiago-Doménech et al. (2008)), and antisense *FaPG1* plants (line APG29, described in Quesada et al. (2009) and Posé et al. (2013)) were grown in a greenhouse under a natural temperature and photoperiod regime. Transgenic ripe fruits showed a strong reduction in *FaplC* or *FaPG1* mRNA levels, higher than 95%. The quality of the ripe fruits at harvest was evaluated using only well-shaped fruits of uniform size and coloration, and weight higher than 5 g. Color was estimated using a chroma meter Minolta CR-400. Soluble solids were measured by using a refractometer Atago N1, and firmness by using a hand-penetrometer (Effegi) with a cylindrical needle of 9.62 mm^2 area. pH was measured in juices extracted from fruits. A minimum of 25 ripe fruits per line were evaluated. The fruits were harvested at the ripe stage, when fully red, frozen in liquid N_2 and stored at -30ºC until used.

2.2. Cell wall extraction and pectin fractionation

The cell walls were extracted from frozen ripe fruits following the protocol of Redgwell, Melton & Brasch (1992) with some modifications, as described by Santiago-Doménech et al. (2008). Briefly, 10-15 frozen fruits were ground to a powder in liquid N_2 and 20 g were homogenised in 40 ml of PAW (phenol: acetic acid: water, 2:1:1, w:v:v). The homogenate was centrifuged at 4000 *g* for 15min and the supernatant filtered through Miracloth (Merck, Bioscience, UK). After centrifugation, the pellet obtained was treated with 90% aqueous DMSO to solubilise the starch. The extract was then centrifuged at 4000 *g* and the pellet washed twice with distilled water. The water fraction was discarded, and the de-starched pellet, the cell wall material (CWM), was lyophilised and weighed.

Pectin fractions were obtained as described by Santiago-Doménech et al. (2008). CWM was washed overnight with deionised water, centrifuged at 6000 *g* for 15 min and the pellet was sequentially extracted with 0.05 M trans-1,2-

diaminocyclohexane-N,N,N'N'-tetraacetic acid (CDTA) in 0.05 M sodium acetate buffer, pH 6, followed by 0.1 M Na_2CO_3 containing 0.1% $NaBH_4$. CDTA extracted polysaccharides (CSP fraction) are those held in the cell wall by Ca^{2+}-mediated crosslinks with the extracts likely to arise primarily from the middle lamellae. Sodium carbonate solubilizes polysaccharides (SSP fraction) held in the wall by ester linkages (Selvendran, 1985; Brummell, 2006) and likely to arise mainly from the primary cell wall. Both pectin fractions were extensively dialyzed and stored until required at -20ºC as aqueous solutions, in order to avoid possible aggregation, which might be induced on freeze-drying.

For neutral sugar analyses, samples from both pectin fractions were extracted with 72% (w/w) sulphuric acid and derivatized to alditol acetates (Blakeney, Harris, Henry & Stone, 1983). The alditol acetates were separated on a Restek Rtx-225 column fitted to a Perkin-Elmer Autosystem XL gas chromatograph equipped with a flame ionization detector.

2.3. Infrared Spectroscopy

Infrared spectra were recorded on a Jasco FT/IR-4100 (Spain) spectrometer coupled to an Attenuated Total Reflectance (ATR) accessory (MIRacle ATR, PIKE Technologies, USA) as previously described in Heredia-Guerrero et al. (2010). Essentially, lyophilized samples were mounted on the ATR crystal and compressed with a clamp and then their absorbance was monitored in the 4000-600 cm^{-1} range at a resolution of 4 cm^{-1} and averaged over 25 scans. Spectra Manager v.2 software (Jasco, Spain) was used to correct for both ATR effect and atmospheric contributions from carbon dioxide and water vapor across the full spectral range.

2.4. ~~Gel Filtration~~ Size exclusion chromatography

The gel filtration chromatography measurements were performed as described previously by Posé et al. (2013). Briefly, ~~250 µl of~~ CSP and SSP pectin fractions were loaded onto a 40 cm height x 10 mm internal diameter column filled with Sepharose CL2B (Sigma–Aldrich Química SA, Spain). Gel medium was equilibrated with 0.2M acetate buffer, pH 5, or 0.05 M TRIS–HCl buffer, pH 8.5, for CSP and SSP samples, respectively. Samples were dissolved in the

corresponding equilibration buffer (6-8 mg ml^{-1}), loaded on the column (250 µl) and eluted at a 14 ml h^{-1} flow rate. Column calibration of the void (V_0) and the total (V_T) volumes were obtained by dextran blue and acetone, respectively. Fractions (1 ml) were collected at a flow rate of 10 ml h^{-1} and assayed for uronic acids (Filisetti-Cozzi & Carpita, 1991).

2.5. Atomic Force Microscopy

AFM samples were prepared following the protocol of Posé et al. (2012). Pectin solutions were diluted to 1-5 µg ml^{-1} in pure water or ammonium bicarbonate buffer 10 mM, pH 8, and dissolved in a hot water bath for 30 min at 80ºC. Then, 3 µl was pipetted onto freshly-cleaved mica (G250, Agar Scientific, UK). The mica surface was dried over a heating block at 37-40ºC for 20 min. The sample was then inserted into the liquid cell of the microscope and visualized under tri-distilled butanol. The mica was mounted in an AFM manufactured by ECS (East Coast Scientific Limited, Cambridge, UK). Short tip AFM contact cantilevers (Budget Sensors, Bulgaria) were used with a resonance frequency of 13 KHz and a quoted force constant of 0.4 Nm^{-1}. The samples were scanned in contact mode at a frequency of 2 Hz. Both topographical and error-signal mode images were collected simultaneously. In excess of 100 images with an area 1 μm^2 were collected for each sample.

2.6. AFM image analysis

The ECS software (SPM 6.01, Cambridge, UK) plane fits and re-normalizes the AFM images and it was used for chain height analysis (Kirby, Gunning, & Morris, 1996). The height of the chains was used to differentiate true branch points from entangled chains (Adams, Kroon, Williamsom & Morris, 2003): overlapping chains show a doubling of height at the crossover point. Further analyses were applied offline. Initially, the original AFM files were converted to TIFF files using Paint Shop Pro v. 5.00 software. Image contrast and stripe correction were optimized using Gwyddion v2.32 software. Contour length measurements, defined as total length including backbone and branches, were analyzed by plotting the length of the chains with the freehand tool of ImageJ software (Adams et al., 2003; Posé et al., 2012). Individual molecules were defined as

strands that were not entangled with, or overlapping other strands, that were long enough to be exactly visualized, and which lay entirely within the scanned area (Adams et al., 2003). In order to obtain reliable results, a minimum of 600 lengths were measured per sample and the results represented as frequency histograms. Number-average (L_N) and weight-average (L_W) contour lengths, as well as polydispersity index (L_W/L_N, PDI) were calculated as described previously (Posé et al., 2012). Additionally, other chain features were analyzed in order to characterize the heterogeneous branch patterns of the chains; including number of branching points per molecule and branch lengths.

2.7. Statistical analysis

The SPSS software (v. 19, IBM Corp. Route 100, Somers, NY) was used for statistical analyses. Fruit characteristics were analyzed by ANOVA and mean separation was done by Tukey test. The Levene test for homogeneity of variances was performed prior to ANOVA. In the case of non-homogeneous variances, the non-parametric Kruskal-Wallis test was used for multiple mean comparisons. In AFM, at least three dozen images and more than 600 individual measurements from each genotype and pectin sample were used to obtain the length distribution representations and statistical parameters. The original data were compared with the Kruskal-Wallis non-parametric median test. Original data were also transformed by natural logarithm to obtain normal distributions, which were compared by ANOVA. The Chi-square test was used to determine differences in the branching of polymer chains and the percentage of micellar aggregates. All statistical tests were performed at $P = 0.05$.

3. Results

3.1. Characteristics of transgenic ripe fruits

At ripening, fruits from both transgenic lines were ~~significantly~~ firmer than control, being the differences statistically significant (Table 1). However, the increase on fruit firmness as result of *FaPG1* silencing was higher than the one achieved in transgenic APEL fruits, 53% vs. 24% in APG and APEL fruits,

respectively. Other parameters related to overall fruit quality, i.e. soluble solids, pH and color, were not modified or showed minor changes in the transgenic lines (Table 1). Fig. S1 (Supplementary data) shows the aspect of control and transgenic plants and fruits.

Table 1. Characteristics of transgenic fruits with *FaplC* (APEL) or *FaPG1* (APG) genes down-regulated by antisense transformation. Fruits were harvested at the stage of full ripeness. Data correspond to mean±SD of a minimum of 25 fruits per line. Means with different letters indicate significant differences by Tukey (soluble solids, pH, color a) or Kruskal-Wallis (firmness, color L and b) tests, both at P=0.05.

	Control	APEL	APG
Firmness (N)	3.3±0.5c	4.1±0.6b	5.0±0.8a
pH	3.5±0.1a	3.4±0.02a	3.5±0.1a
Soluble solids (^{o}Brix)	7.7±1.6a	8.3±1.4a	7.6±1.5a
Color			
L	37.3±2.7a	39.9±6.4a	35.7±3.0b
a	37.4±4.5b	40.1±3.4a	36.5±3.7b
b	20.2±3.3b	25.2±7.0a	19.2±3.6b

3.2. FTIR analysis of fruit pectins

ATR-FTIR spectra of CDTA (CSP) and sodium carbonate (SSP) soluble pectins in control and transgenic lines are shown in Fig.1. Both fractions showed absorption bands in the mid-infrared region, 1200-800 cm^{-1}, typical of polyuronide samples rich in polygalacturonic acid. These bands are due to ring vibrations overlapping with stretching vibration of the hydroxyl groups and the glycosidic bond vibration, and can be used to identify polysaccharide mixtures with different composition. When CSP fractions are compared with SSP, the later showed an increase in the absorbance at 1075, 1047 and 953 cm^{-1} and a decrease

in the peak at 1100 cm^{-1}, suggesting different sugar compositions: the SSP pectin is enriched in neutral sugars. No differences were detected in this region between the control and transgenic samples, either for the CSP or SSP samples, indicating that the pectinase silencing did not modify the neutral carbohydrate composition. These results were confirmed by neutral sugar analysis using gas chromatography (Table 2).

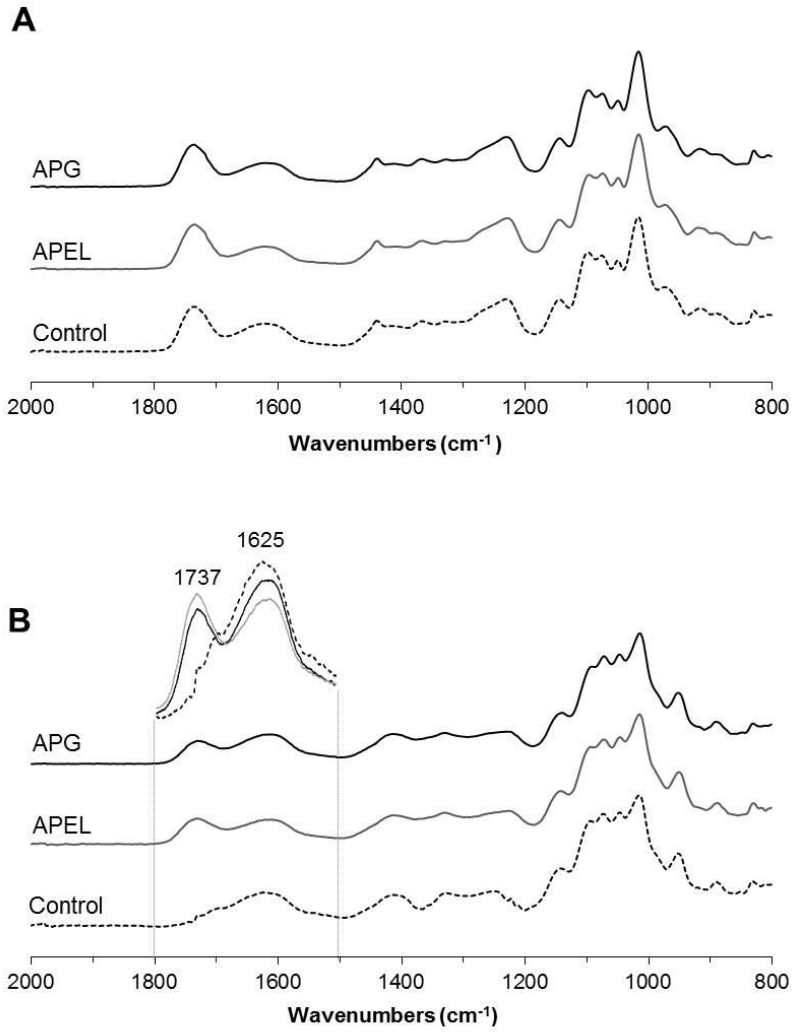

Figure 1. ATR-FTIR spectra of CDTA (A) and sodium carbonate-soluble (B) pectin fractions in the 2000-800 cm^{-1} region. Pectins were extracted from ripe fruits of Control, *FaplC* (APEL) and *FaPG1* (APG) antisense transgenic lines (dashed, grey and black lines respectively). Inlet in Fig. 1-B shows detailed peaks of esterified (~1737 cm^{-1}) and desterified (~1625 cm^{-1}) carboxyl groups, displaying both transgenic lines a recalcitrant pool of esterified residues.

Table 2. Neutral sugar content in CDTA (CSP) and sodium carbonate (SSP) soluble pectins from fruits with *FaplC* (APEL) or *FaPG1* (APG) genes down-regulated. Values correspond to mean±SD of three independent replicates.

		Neutral sugar (mol%)						
		Rha	Fuc	Ara	Xyl	Man	Gal	Glc
CSP	Control	7.2±0.03	1.3±0.5	33.7±0.2	4.1±0.2	3.7±0.8	47.9±1.5	2.0±0.7
	APEL	7.6±0.5	1.2±0.1	32.3±1.2	4.4±0.1	4.0±0.5	48.2±1.7	2.4±0.3
	APG	7.3±1.1	1.1±0.3	33.7±0.1	3.5±0.9	4.8±1.8	47.6±1.7	3.5±0.9
SSP	Control	4.8±0.2	0.6±0.02	27.7±0.3	2.7±0.1	1.5±0.2	61.7±0.1	1.0±0.1
	APEL	5.0±0.03	0.5±0.01	28.5±0.3	2.5±0.1	1.4±0.2	61.3±0.02	0.8±0.04
	APG	4.4±0.6	0.4±0.1	28.7±0.1	2.3±0.2	1.1±0.2	62.4±1.2	0.7±0.1

The relationship between peaks at ~~1740~~ 1737 cm^{-1}, assigned to ~~C=C~~ C=O stretching vibration of methyl esterified carboxylic groups, and 1625 cm^{-1}, corresponding to the symmetrical stretching vibration of COO^- group, can be used to estimate the degree of methyl esterification in the pectin samples (Manrique & Lajolo, 2002). In the CSP samples, no differences between wild type and transgenic lines were detected in the intensities of these absorption bands suggesting a similar degree of methylation (Fig. 1A). As expected, the peak at ~~1740~~ 1737 cm^{-1} disappeared whereas peaks at 1625 and 1415 cm^{-1} increased in SSP samples from control fruits, due to the elimination of ester linkages during the alkaline extraction procedure (Fig. 1B). However, the SSP pectin fractions isolated from both transgenic genotypes still maintained a strong absorption band at ~~1740~~ 1737 cm^{-1} (Fig. 1B~~, inlet~~), indicating the presence of some ester bonds resistant to the mild alkaline conditions. Finally, the low absorption at 1670 and 1588 cm^{-1} for amide bands, indicates an absence or undetectable presence of protein in both pectin fractions.

3.3. ~~Molecular mass profiles of bulk polymers by GFC~~ Size exclusion chromatography of bulk pectic polymers

Pectin size modifications induced by the inhibition of *FaplC* or *FaPG1* genes were different. CDTA soluble pectins from the wild type fruits showed a profile consisting of three peaks, which corresponded to three main groups of polymers distributed throughout the eluted volume. The peak corresponding to the middle-sized pectic polymers, eluting at 22 ml, was the most abundant (Fig. 2A). APG samples showed a similar profile, but, in this case, an increased abundance of larger polyuronides was observed in the first peak, eluting at 16 ml (Fig. 2B). By contrast, APEL samples displayed a completely different profile with a main prominent peak in the middle of the elution profile, showing a main pool of middle-sized pectins (Fig. 2A). On the other hand, sodium carbonate soluble fractions showed profiles with a main pool of low molecular size polymers that eluted at 28 ml, close to the total volume (Fig. 2C, D). This peak was shifted to the left in both transgenic samples when compared to the wild type control (Fig. 2C, D). This shift indicates a higher molecular mass in both of the transgenic samples than in the wild type, revealing a lesser degree of depolymerisation in the transgenic lines. Furthermore, both transgenic samples also included an extra peak near the void volume that was not present in the wild type, this peak being more prominent in the APEL samples (Fig. 2D).

3.4. Nanostructural analysis of pectins by AFM

The ability to analyze isolated polymer chains is the main advantage of the AFM technique, when compared with bulk analysis by ~~GFC~~ SEC, which allows unraveling of a further level of pectin matrix complexity. AFM visualization not only allows measurement of contour lengths from isolated chains, but also provides valuable topographical information in order to differentiate between true branched points and entangled chains. In general, AFM scanning of highly diluted strawberry pectin extracts, in the range 10^{-6} g cm^{-3}, showed isolated fibrous structures with linear chains as the main feature and some aggregates (Supplementary Data, Fig. S2A). True branched points have the same height than isolated chains (Fig. S2B, profile 1). The aggregates were identified because they displayed higher heights than isolated chains (Fig. S2B, profile 2). They were also

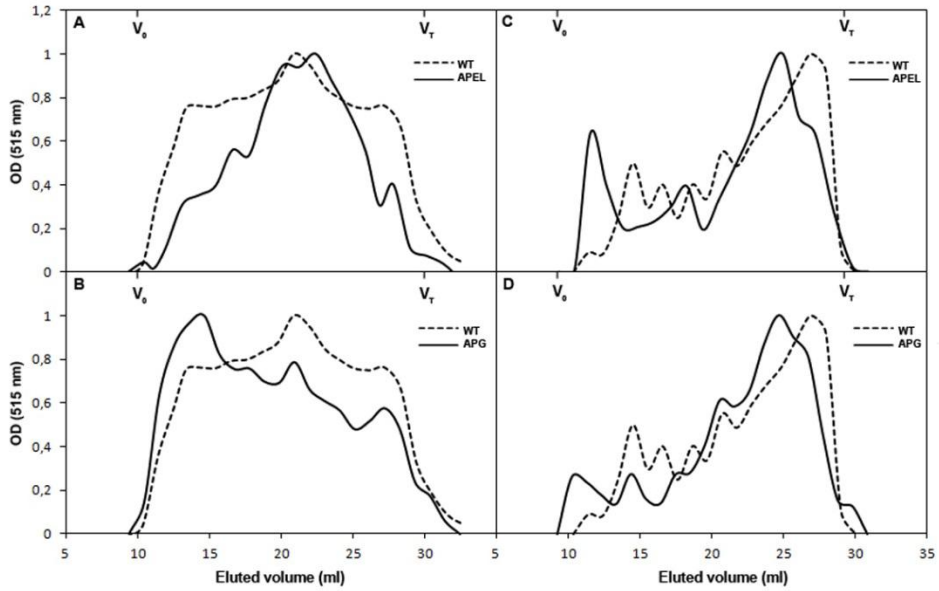

411

412

413 **Figure 2.** ~~Molecular mass~~ Chromatographic elution profiles of polyuronides
414 extractable by CDTA (A, B) and sodium carbonate (C, D) from cell walls of wild-
415 type, antisense *FaplC* (APEL; figures A,C) and antisense *FaPG1* (APG; figures
416 B,D) ripe fruits. Profiles were obtained by ~~gel filtration~~ size exclusion
417 chromatography on Sepharose CL-2B. Columns were calibrated by dextran blue
418 and acetone for void volume (V_0) and total volume (V_T), respectively. Fractions
419 were assayed for uronic acid and expressed as relative optical density (OD) at 515
420 nm. The results show the average profile of at least two independent
421 chromatographic assays per sample.

422

423

424 present even at low sample dilution when few isolated individual chains were
425 present in the sample. This suggests that aggregates are not formed by casual
426 overlapping of individual chains as result of the sample processing for AFM but
427 are multi-polymer complexes held together by intermolecular interactions.
428 Interestingly, aggregates often exhibited a defined structure having a core middle
429 point of higher height with emerging strands (Fig. S2 ~~Fig. 3~~). Similar structures
430 have previously been observed in other species and described as micellar like
431 structures (Kirby, MacDougall, & Morris, 2008; Morris, Gromer, & Kirby, 2009;
432 Posé, Kirby, Mercado, Morris, & Quesada, 2012). Figs. 3 and 4 show typical
433 AFM images of CDTA and carbonate extracted polysaccharides, respectively,

isolated from ripe fruits from wild-type and both transgenic lines. In general, CSP pectins were larger than SSP polymers. A low proportion of branched chains and small aggregates were also present in the samples. Qualitatively, AFM images showed more complex nano-structural patterns in chains isolated from transgenic lines, both multi-branched molecules and micellar aggregates were more abundant in these samples than in controls, either in CSP (Fig. 3) or SSP samples (Fig. 4).

Contour lengths of several dozen isolated chains were recorded. Length measurement from topographical AFM images provides enough information to generate the characteristic position parameters L_N, L_W and the polydispersity index (PDI) for the shape of contour length distributions (Round, MacDougall, Ring, & Morris, 1997; Round, Rigby, MacDougall, Ring, & Morris, 2001). Histograms for the length distribution for CSP samples were in the range 20-650 nm whilst SSP distribution ranged between 20 and 500 nm (Fig. 5). Both sets of data were right-skewed and showed a good fitting to log-normal distributions (Fig. 5). Table 3 shows the histogram parameters in CSP and SSP polymers from control and transgenic lines. The median, as a more appropriate average for asymmetrical distributions, was used to compare length distributions statistically. In the case of CSP samples, antisense *FaPG1* fruits showed the highest L_N, L_W and PDI values, with the median value of the length distributions being statistically higher than the value obtained for the control. CSP samples from antisense pectate lyase fruits showed an intermediate distribution of lengths between APG and wild type. Polymers soluble in sodium carbonate were shorter than those solubilized with CDTA, as previously described by Posé et al. (2012) for ripe strawberry fruits. When the three genotypes were compared, the SSP chains from the APG fruits were also significantly longer than the wild type, with the APEL polymers showing an intermediate length between APG and wild type (Table 3). The differences in CSP and SSP polymer lengths among the genotypes studied can be easily visualized when the results are plotted as cumulative frequencies (Fig. 5 D,H). Log-normal transformation of contour length data were also applied to compare statistically wild type and transgenic samples, as previously described by Posé et al. (2012), obtaining similar conclusions to those described above.

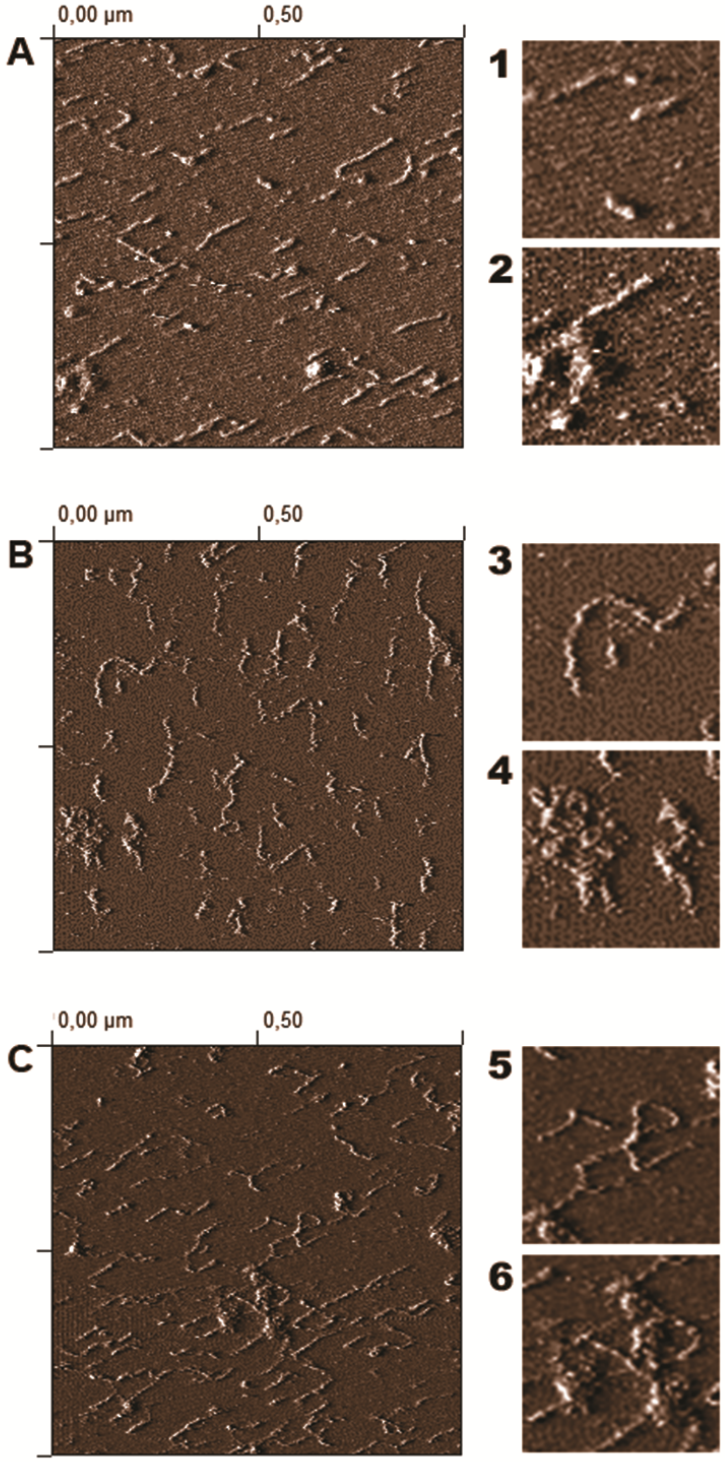

Figure 3. Typical AFM images, in topographical mode, of ~~CDTA~~CSP-pectin samples from cell walls of wild-type (A), antisense *FaplC* (B) and antisense *FaPG1* (C) ripe fruits. Images 1-6 correspond to zoomed areas to show unbranched isolated chains (1,3), branched isolated molecules (5) and micellar aggregates (2,4,6). Scan size: 1 µm (A-C) and 250 nm (1-6).

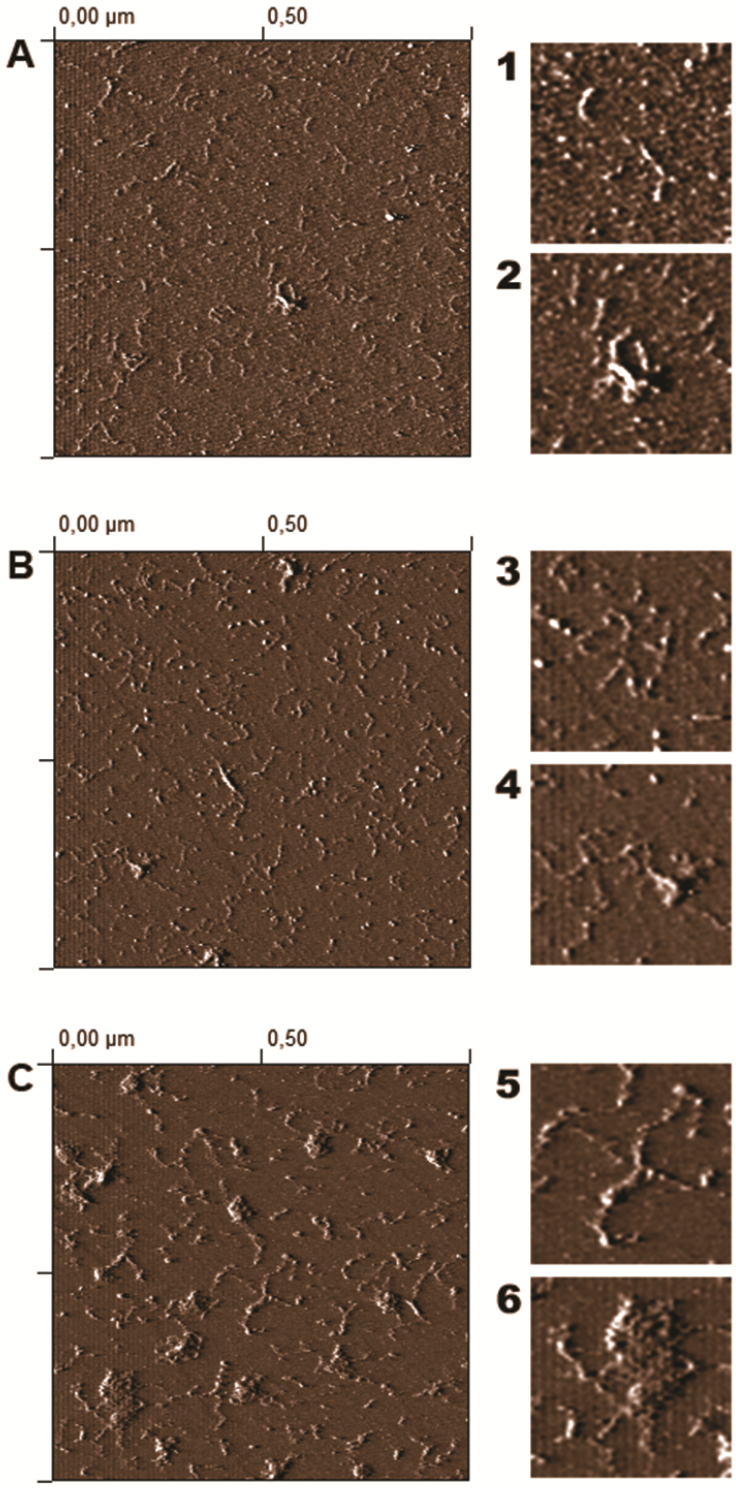

528 **Figure 4**. Typical AFM images of carbonateSSP-pectin samples from cell walls of
529 wild-type (A), antisense FaplC (B) and antisense FaPG1 (C) ripe fruits. Images 1-
530 6 correspond to zoomed areas to show unbranched isolated chains (1), branched
531 molecules (3,4,5) and micellar aggregates (2,6). Scan size: 1 µm (A-C) and 250
532 nm (1-6).

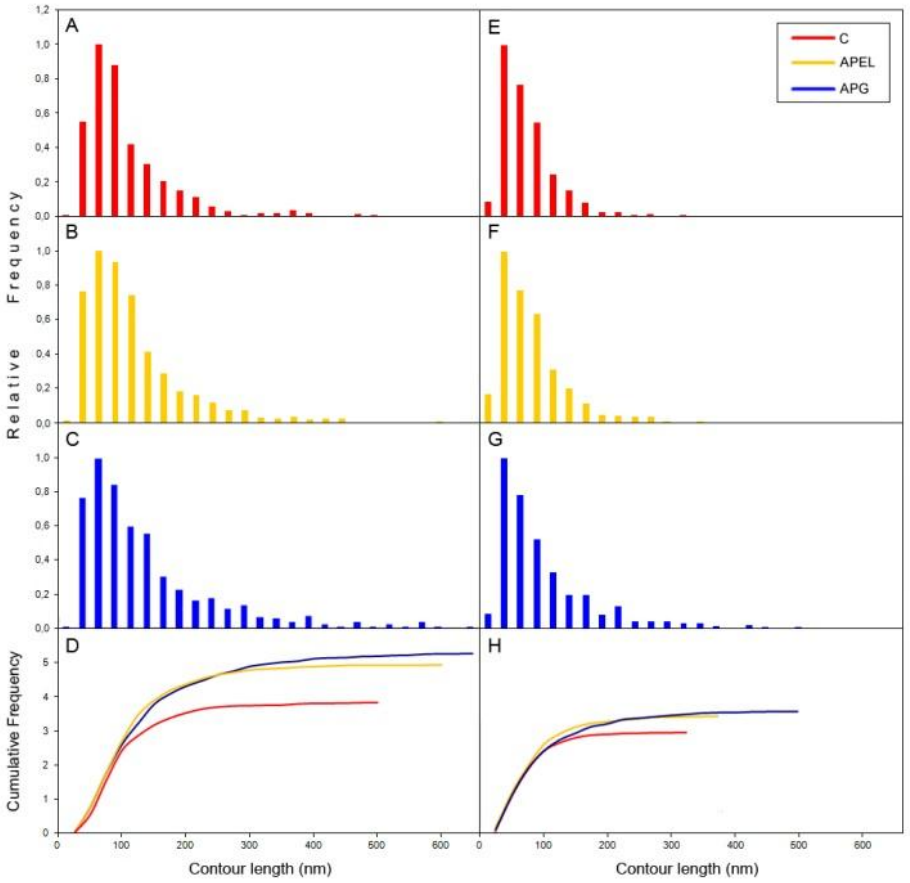

Figure 5. Contour length distribution of CDTA (CSP) and sodium carbonate (SSP) soluble polymers isolated from fruit cell walls of control (A, E), antisense *FaplC* (APEL; figures B, F) and antisense *FaPG1* (APG; figures C, G) ripe fruits. Bars represent relative frequencies of the observed data ~~whilst the curved lines represent Log normal approximations~~. (D, H) Cumulative frequencies for CSP (D) and SSP (H) fractions, normalized to the maximum frequency value.

Table 3. AFM characterization of pectins chains in fruits with *FaplC* (APEL) or *FaPG1* (APG) genes down-regulated. Pectins were extracted from ripe strawberry fruits from control and transgenic lines and analysed by AFM in contact mode. Descriptors of contour length distributions (number-average (L_N), weight-average (L_W) and polydispersity index (PDI)) of CDTA (CSP) and sodium carbonate (SSP) soluble pectins obtained from AFM images. ME corresponds to the median value of original data. Within each pectin fraction, median values followed by different letters are significantly different by non-parametric median test at P=0.05. N = 710, 734 and 660 for Control, APEL and APG CDTA samples, and N = 673, 608 and 527 for Na_2CO_3 samples, respectively.

		L_N (nm)	L_W (nm)	PDI	ME (nm)
CSP	Control	103.2	147.1	1.42	84.0 b
	APEL	112.4	164.3	1.46	93.5 a
	APG	132.8	211.7	1.59	101.0 a
SSP	Control	72.3	97.7	1.35	61.0 b
	APEL	80.4	117.7	1.46	67.5 ab
	APG	96.9	156.2	1.61	71.0 a

In addition to changes in the length of the pectin chains, antisense silencing of both pectinase genes also induced a modification of the chain branching pattern. An increased percentage of branched molecules, as well as multi-branched polymers, were observed in the two pectin fractions isolated from APG fruits when compared to wild type (Table 4). In the APEL line, CSP polymers showed a similar branching pattern than control, but SSP polymers displayed a higher percentage of ramifications than the wild type, with the percentage of branching molecules found to be slightly lower than observed in the APG samples (Table 4). With regard to branch lengths, the CDTA fractions showed no significant differences amongst the different lines. By contrast, the carbonate soluble pectin

574 fraction from the APG line had significantly longer branches than the APEL and
575 wild type lines (Table 4).
576 Finally, in the control samples the number of micellar-like aggregates per
577 scanned area was similar in the CSP and SSP pectin fractions (Fig. 6). By contrast,
578 in both transgenic samples, the presence of aggregates was higher in SSP samples
579 and these values were significantly higher than those found in the control SSP
580 fraction. The highest presence of aggregates was observed in both APG fractions.
581 In summary, the quantitative analysis of the AFM images indicates that the
582 silencing of both pectinases increases not only the length of the pectin molecules
583 but also their complexity, reflected in the higher percentage of branched
584 molecules and the increased number of supra-molecular complexes. Furthermore,
585 these differences were more conspicuous in pectin fractions from *FaPG1* silenced
586 fruits than in fractions from *FaplC* down-regulated fruits.
587

588 **Table 4.** AFM characterization of pectin branches in fruits with *FaplC* (APEL) or
589 *FaPG1* (APG) genes down-regulated. Pectins were extracted from ripe strawberry
590 fruits from control and transgenic lines and analysed by AFM in contact mode.
591 Branch length distribution parameters (number-average (L_N), weight-average (L_W)
592 and polydispersity index (PDI)) and branching pattern of CDTA (CSP) and
593 sodium carbonate (SSP) soluble pectins obtained from AFM samples. ME
594 corresponds to the median value of original data. Branching was defined as the
595 percentage of branched molecules per total number of molecules. Multibranching
596 was defined as the percentage of polymers with more than one branch per
597 branched molecules. Within each pectin fraction, median values followed by
598 different letters are significantly different by the non-parametric median test at
599 P=0.05. Chi-square test was used for branching percentages. N = 52, 53 and 118
600 for Control, APEL and APG CDTA samples, and N = 63, 87 and 94 for Control,
601 APEL and APG for Na_2CO_3 samples.
602

		Branch parameters				Branching pattern (%)	
		L_N (nm)	L_W (nm)	PDI	ME (nm)	Branching	Multibranching
CSP	Control	57.8	84.3	1.46	48.0a	7.3b	1.9b
	APEL	63.4	87.0	1.37	54.0a	7.2b	5.7b
	APG	63.8	86.6	1.36	51.0a	17.9a	21.2a
SSP	Control	34.1	43.5	1.27	29.5b	9.4b	4.8b
	APEL	33.3	47.5	1.44	28.0b	14.3a	13.8a
	APG	51.7	67.9	1.31	41.0a	17.9a	20.2a

603
604
605
606
607
608
609

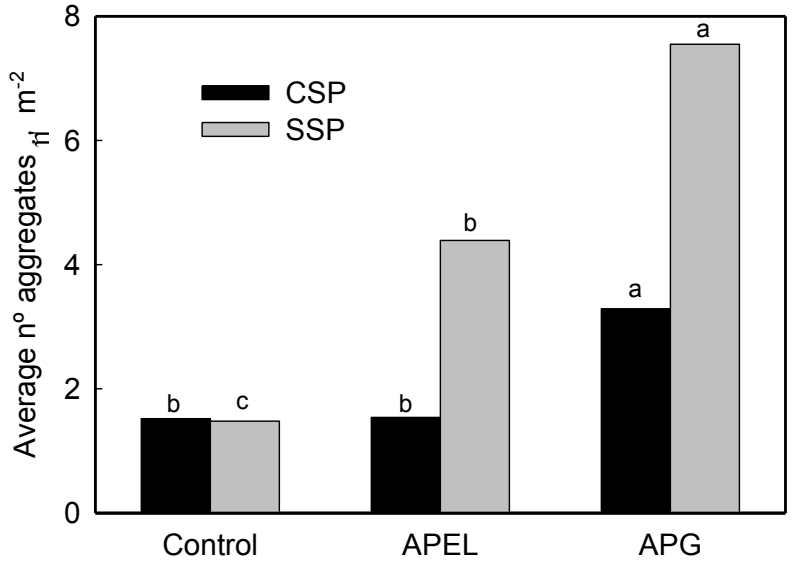

610
611

612 **Figure 6.** Average number of micellar aggregates in CDTA (CSP) and sodium
613 carbonate (SSP) soluble pectin samples isolated from cell walls of control,
614 antisense *FaplC* (APEL) and antisense *FaPG1* (APG) ripe fruits. For each pectin
615 sample, bars with different letters indicate significant differences by Tukey test at
616 *P*=0.05.

617
618

619 **5. Discussion**

620

621 The functional analyses of pectin degrading genes in fruits with extremely
622 different textural properties, such as strawberry and apple, have reopened the
623 debate about the role of pectin disassembly in fruit softening (Jiménez-Bermúdez
624 et al., 2002; Quesada et al., 2009; Atkinson et al., 2012). In an attempt to relate
625 disassembly at the nanostructural level with fruit softening, we have analyzed
626 pectin samples isolated from plants with a pectate lyase or a polygalacturonase
627 gene silenced, since both genotypes showed a significant increase in fruit
628 firmness. Additionally, we have already demonstrated in these genotypes that
629 pectins ionically bound to the cell wall, extracted with CDTA (CSP), and
630 covalently bound to the wall, sodium carbonate soluble pectins (SSP), displayed
631 extensive biochemical changes when compared with wild type fruits (Santiago-

Doménech et al., 2008; Posé et al., 2013).

5.1. FTIR spectra and ~~GFC~~ SEC analysis of transgenic pectin samples

The mid-infrared region at 1200-800 cm^{-1} in FTIR spectra is used to identify particular polysaccharides (Filippov, 1992; Largo-Gosens et al., 2014). In this region, the CSP and SSP spectra from strawberry cell walls showed a maximum peak at 1016 cm^{-1}, being indicative of pectin samples enriched in polygalacturonic acid. However, different intensities in several bands within this region seen for the CSP and SSP samples, suggest a higher proportion of neutral sugars in the SSP polysaccharides (Coimbra, Barros, Barros, Rutledge & Delgadillo, 1998; Kacuráková, Capek, Sasinková, Wellner & Ebringerová, 2000), which is in accordance with the major presence of RGI in extracts solubilised by sodium carbonate (Brummell, 2006). The silencing of both pectinase genes did not modify the neutral sugar composition within the cell wall fractions. Similarly, the degree of esterification in CSP pectins, estimated by the ratio of the peaks ~~areas of the ester bands~~ at 1745 and 1630 cm^{-1} (Manrique & Lajolo, 2002), was not altered in the transgenic genotypes. The most striking difference between the control and the transgenic samples was the presence of some ester bonds resistant to mild alkaline extraction conditions in the transgenic SSP pectins, resulting in the presence of an absorption band at about ~~1740~~ 1737 cm^{-1} despite the alkaline extraction. These ester bands could be ascribed to phenolic esters, since the detailed observation of FTIR spectra of transgenic SSP pectins exhibited a shoulder at 1720 cm^{-1} in the ester band (Fig. 1B ~~inlet~~) that is characteristic of aromatic esters (Séné, McCann, Wilson, & Grinter, 1994; Largo-Gosens et al., 2014). Alternatively, acetyl (Marry et al., 2006) and/or borate (O'Neill et al., 2004) esters could also contribute to the ester band fingerprint observed in the transgenic samples, but further research is required to ascertain the exact nature of these ester bands

The bulk analysis of pectins by ~~gel filtration chromatography~~ SEC revealed important differences in polymer size distribution between *FaPG1* and *FaplC* transgenic cell walls. *FaPG1* CSP samples displayed larger average molecular weights than the control due to an increase in the relative abundance of polyuronides of large molecular mass which eluted in the peak close to the void volume. However, *FaplC* down-regulated fruits showed an increase on middle-

size pectins. In the case of sodium carbonate soluble pectins, both transgenics showed a similar displacement to the left of the main peak, eluting in control fractions at 26 ml, and also an increased amount of polyuronides, eluting at 10ml, that were not present in the control. This peak, which corresponds to a molecular mass very close to the void volume of the column, was significantly more abundant in APEL fruits. The absence of this peak in control samples might indicate that these polyuronides were depolymerized during ripening, leading to the two peaks that appeared at 14 and 17 ml in control profile. Alternatively, the peak of large molecular mass that was absent in the CDTA profile of APEL fruits might correspond to the strong peak that appears at the same eluting volume in the SSP profile, since it has been suggested that pectate lyase solubilizes subsets of strongly bound pectins (Santiago-Doménech et al., 2008).

5.2. AFM analysis of pectin samples revealed longer and more branched polymers as a result of pectinase silencing

Isolated pectin chains from the three genotypes were studied at the nano-structural level by AFM. As observed previously in strawberry, peach and tomato fruits, CSP pectin chains were larger than SSP ones (Round et al., 2001; Kirby et al., 2008; Yang, Chen, An, & Lai, 2009; Posé et al., 2012). In general, number–average (L_N) and weight–average (L_W) contour length values for both pectin fractions were in the same range of those reported for equivalent pectin fractions isolated from mature green tomato and sugar beet (Kirby et al., 2008; Round, Rigby, MacDougall, & Morris, 2010). However, much longer pectin chains (>1000 nm) have been observed in other fruits, i.e. peach (Yang et al., 2009), jujube (Wang et al., 2012) and apricot (Chen et al., 2013). As regard the effect of pectinase silencing on pectin nanostructure, AFM images illustrated the increase in the size of CSP and SSP pectic chains from both transgenic fruits. The silencing of *FaplC* gene increased L_N and L_W contour length values from CSP and SSP samples in a similar magnitude, in the range of 9-20%, when compared with wild type. Down-regulation of *FaPG1* had a stronger effect on pectin length, with L_N and L_W, on average, 31 and 51% higher than the control values, respectively. Interestingly, the increment on pectin length induced by PG silencing was slightly higher in SSP than in CSP.

The number of carbohydrate residues as well as molecular mass of the pectic structures visualized by AFM can be estimated from L_N and L_W values considering a 3_1 helix structure with a pitch of 1.34 nm from fibre diffraction analysis of polygalacturonic acid (Walkinshaw & Arnott, 1981). According to this assumption, the degree of polymerization (DP) of control pectins was approximately 231 and 161 residues for CSP and SSP fractions, respectively. These values are slightly lower than those reported by Round et al. (2010) for mature green tomato pectins extracted with sodium carbonate. The number of residues was significantly increased in APG samples, 297 and 217 DP, for CSP and SSP respectively, showing pectic chains from APEL fruits an intermediate number of residues. It has been estimated that HG domains, obtained after fruit pectin hydrolysis with 1N HCl, are about 72-117 DP (Thibault, Renard, Axelos, Roger & Crépeau, 1993; Yapo, Lerouge, Thibault, & Ralet, 2007), whereas RG-I isolated backbone is about 70-80 DP (Yapo et al., 2007). The chains depicted in this study by AFM must account on more than one of those pectin domains. On the other hand, although both the AFM and ~~GFC~~ SEC studies support diminished pectin degradation due to *FaPG1* or *FaplC* silencing, it is not possible to make a direct comparison of the average molecular mass obtained for the pectic polymers resolved in chromatography with those deduced from AFM images. AFM depicts nanostructural details on isolated pectic chains while GFC monitors the volume of the molecules in a complex mixture, based on hydrodynamic behaviour of polymers through a porous gel matrix. Thus, longer and more branched pectin and further micellar aggregations depicted by AFM could develop a more 'bulky' pectin mixture, as is revealed by ~~GFC~~ SEC.

In addition to pectin length, the branching patterns of the pectins were also modified in the two transgenic genotypes analysed, especially in the case of *FaPG1* silenced fruits. Both pectin fractions isolated from these fruits showed a higher number of branches that were also longer than those observed in the control in the case of SSP. By contrast, APEL lines only showed a higher branching percentage than control in the sodium carbonate soluble fraction and the branch length was not modified. Round et al. (1997) observed that almost 20% of single polymers from sodium carbonate pectins from mature green tomato visualized by AFM showed long branches, with approximately 30% of these

731 having more than one branch. Yang et al. (2009) suggested a relationship between
732 peach firmness and pectin nanostructure, since crisp cultivars showed longer and
733 more branched CSP and SSP polymers than soft fruits. In apricot and peach it has
734 also been observed that there is a reduction in branching during post harvest
735 storage of fruits (Yang, An, Feng, Li, & Lai, 2005; Liu et al., 2009). Recently,
736 AFM in pear fruits (Zdunek, Koziol, Pieczywek & Cybulska, 2014) also found a
737 higher branching index on CSP fractions in the firmer cultivar.
738 The physicochemical nature of linear chain branches is unclear. Neutral sugar
739 composition and linkage analyses suggested that the branches observed by AFM
740 in pectin chains do not correspond to neutral sugars but to polygalacturonic acid
741 attached to the pectin backbone via an undetermined branch point, with the
742 neutral sugars present as short branches undetected by AFM (Round et al., 2001).
743 This hypothesis was supported by experiments evaluating the effect of mild acid
744 hydrolysis on SSP pectins from unripe tomato (Round et al., 2010). This treatment
745 sequentially releases carbohydrate residues present in polyuronides at different
746 rates, Ara, Gal and Rha linkages being the most labile and GalA the most resistant
747 (Thibault et al., 1993). Round et al. (2010) observed that almost complete
748 hydrolysis of Ara, Gal and Rha had no significant effect on backbone and branch
749 length distributions in individual pectins visualized by AFM. The present results
750 indicate a higher branching when pectinases targeting HGA backbone are silenced
751 and they also support a polygalacturonic acid composition of the branches.
752 Transgenic fruits also displayed a higher number of micellar aggregates than
753 the control, especially in the case of *FaPG1* antisense fruits. Similar structures
754 have previously been described by AFM in tomato and sugar beet (Kirby et al.,
755 2008; Morris et al., 2009). It has been suggested that these complexes may contain
756 irreducible HGA linked to RG-I, since their size decreased upon acid hydrolysis in
757 parallel to neutral sugars lost (Round et al., 2010). As previously observed in
758 tomato pectins (Round et al., 2010), micellar aggregates from strawberry fruits
759 were often visualized with emerging strands with similar dimensions to isolated
760 chains. It is therefore probable that some of these HGA chains could be originally
761 linked to aggregates containing RG-I by bonds which would be broken during
762 ripening induced cell wall disassembly, and/or artificially during cell wall
763 chemical extraction or pectin fractionation. This interpretation of the aggregates

appearance is also in agreement with conformational studies performed in isolated RG-I. The Rha units of the RG-I backbone, as well as the neutral sugar side chains, confer a notable level of flexibility to this macromolecule, usually resulting in the formation of very compact or sphere-like macromolecules in contrast to the extended stiff rod-like conformation of HGA (Yapo, 2011).

5.3. A hypothesis about the role of *FaPG1* and *FaplC* on strawberry fruit softening

Fig. 7 shows a hypothetical mode of action of these two enzymes as deduced from the results described above. Pectate lyase would act in restricted and more localized microdomains in the primary cell wall reducing HGA backbone length and the number of chain branches. This enzyme would play a minor role in the degradation of middle lamella pectins extracted with CDTA. *FaPG1* protein, by contrast, would have a wider spread and more pronounced activity than *FaplC* during strawberry ripening, degrading HGA backbone and reducing the number of side-chains of middle lamella and primary cell wall polymers. Furthermore, this protein also seems to act reducing the length of side-chains from pectin covalently bound to the cell wall. The lesser effect of *FaplC* downregulation on CDTA pectins may be due to an esteric hindrance and/or restricted mobility of the *FaplC* enzyme within the primary cell wall, as has been suggested from immunolocalization studies of pectate lyase proteins (Benítez-Burraco et al., 2003). Differences in apoplastic pH could also contribute. During strawberry ripening, pH decrease from 5 to 3 is observed (Moing et al., 2001), a pH value far from the optimal pH for pectate lyase activity that is near to 8.5 (Sénéchal et al., 2014). In addition to the effect on HGA, the silencing of both enzymes seems to limit RG-I degradation, especially in the case of *FaPG1* plants. RG-I plays a central function in the primary cell wall as a scaffold to which other pectic polysaccharides, mainly HGA and RG-II, may be covalently attached to form the pectin matrix which determines cell wall strength and mechanical properties (Yapo, 2011). Our hypothesis is that the silencing of *FaPG1* or *FaplC* not only preserved HGA from degradation, as deduced from the more branched and longer length of isolated chains, but would also reduce RG-I disassembly, reflected in a higher density of aggregates in transgenic samples.

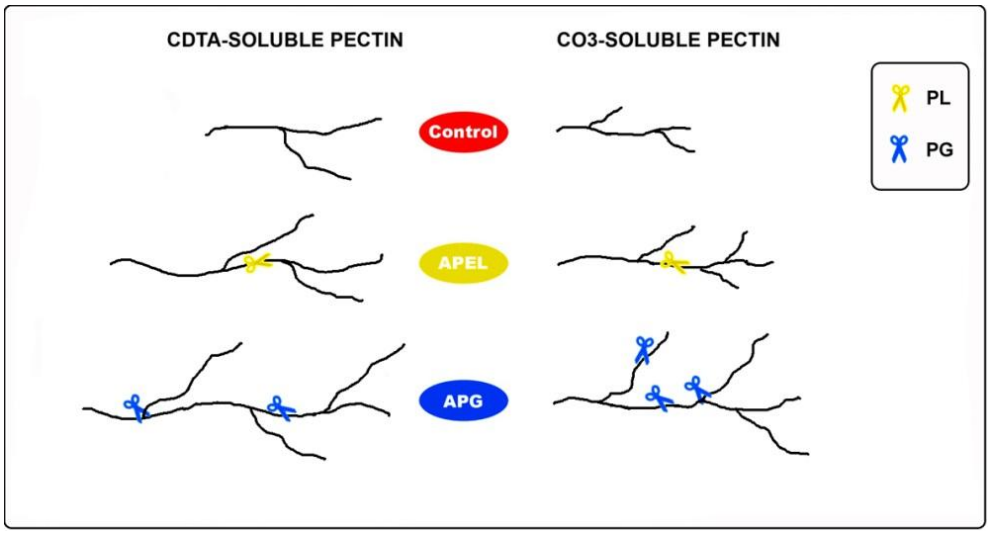

Figure 7. Schematic representation of a hypothetical mode of action for pectate lyase and polygalacturonase on CDTA and sodium carbonate pectin chains during strawberry ripening based on AFM analysis of antisense *FaplC* (APEL) and *FaPG1* (APG) ripe fruits. Length of pectin chains and branches, as well as the number of branches per chain are drawing at scale. Scissors indicate putative points of cutting for both enzymes. Pectate lyase would reduce HGA backbone length and the number of chain branches. This enzyme might play a minor role in the degradation of middle lamella pectins extracted with CDTA. Polygalacturonase has a more pronounced activity during strawberry ripening, degrading HGA backbone, and reducing the number of side-chains of pectins from both polyuronide fractions, as well as the length of sodium carbonate pectin side-chains.

6. Conclusions

The silencing of polygalacturonase and pectate lyase genes reduced pectin degradation during strawberry fruit softening, as confirmed both by ~~GFC~~ SEC ~~or~~ and AFM analysis. The results obtained suggest that each pectinase acts on specific pectin domains. In particular, polygalacturonase induced significant pectin disassembly of polyuronides from both the middle lamella and primary cell wall, whereas pectate lyase had a more limited effect, restricted mainly to pectins covalently bound to the cell wall. These results correlate nicely with the firmer phenotype of APG fruits when compared with fruits with down-regulated pectate

lyase. In summary, the fine structure elucidation of isolated pectins from transgenic strawberry fruits revealed that, apart from the increased length, other pectin features such as side chains distribution and aggregation status were modified as result of pectinase silencing. It would be interesting to address whether these effects are direct or side effects of pectinase action. Globally, these structural features contribute to the reinforced mechanical strength of cell walls for both transgenic fruits and support the load-bearing capacity of the pectin matrix.

Acknowledgements: This work was supported by the Ministerio de Economía y Competitividad of Spain and Feder European Union Funds (grant reference AGL2011-24814). The research at IFR was supported through the BBSRC core grant to the Institute. CP was supported with a FPI fellowship from the Spanish Government (grant reference BES-2009-027985).

References

Adams, E. L., Kroon, P. A., Williamson, G., & Morris, V. J. (2003). Characterisation of heterogeneous arabinoxylans by direct imaging of individual molecules by atomic force microscopy. *Carbohydrate Research*, *338*, 771-780.

Atkinson, R. G., Sutherland, P. W., Johnston, S. L., Gunaseelan, K., Hallett, I. C., Mitra, D., Brummell, D. A., Schröder, R., Johnston, J. W., & Schaffer, R. J. (2012). Down-regulation of *POLYGALACTURONASE1* alters firmness, tensile strength and water loss in apple (*Malus x domestica*) fruit. *BMC Plant Biology, 12*, 129-142.

Benítez-Burraco, A., Blanco-Portales, R., Redondo-Nevado, J., Bellido, M. L., Moyano, E., Caballero, J. L., & Muñoz-Blanco, J. (2003). Cloning and characterization of two ripening-related strawberry (*Fragaria* x *ananassa* cv. Chandler) pectate lyase genes. *Journal of Experimental Botany, 54,* 633-645.

Blakeney, A. B., Harris, P. J., Henry, R. J., & Stone, B. A. (1983). A simple and rapid preparation of alditol acetates for monosaccharide analysis. *Carbohydrate Research, 113*, 291-299.

Brummell, D. A. (2006). Cell wall disassembly in ripening fruit. *Functional Plant Biology, 33*, 103-119.

Brummell, D. A., & Harpster, M. H. (2001). Cell wall metabolism in fruit softening and quality and its manipulation in transgenic plants. *Plant Molecular Biology, 47*, 311-340.

Chen, Y., Chen, F., Lai, S., Yang, H., Liu, H., Liu, K., Bu, G., & Deng, Y. (2013). In vitro study of the interaction between pectinase and chelate-soluble pectin in postharvest apricot fruits. *European Food Research and Technology, 217*, 1438-2377.

Coimbra, M. A., Barros, A., Barros, M., Rutledge, D. N., & Delgadillo, I. (1998). Multivariate analysis of uronic acid and neutral sugars in whole pectic samples by FT-IR spectroscopy. *Carbohydrate Polymers, 37*, 241-248.

Fabi, J. P., García-Broetto, S., García Leme da Silva, S. L., Zhong, S., Lajolo, F. M., & Oliveira do Nascimento, J. R. (2014). Analysis of papaya cell wall-related genes during fruit ripening indicates a central role of polygalacturonases during pulp softening. *PLOS One, 9*, e105685.

Filisetti-Cozzi, T. M. C. C., & Carpita, N. C. (1991). Measurement of uronic acids without interference from neutral sugars. *Analytical Biochemistry, 197*, 157-162.

Filippov, M. P. (1992). Practical infrared spectroscopy of pectic substances. *Food Hydrocolloid, 6*, 116-142.

Goulao, L. F., & Oliveira, C. M. (2008). Cell wall modification during fruit ripening: when a fruit is not the fruit. *Trends in Food Science and Technology, 19*, 4-25.

Hadfield, K. A., & Bennett, A. B. (1998). Polygalacturonases: many genes in search of a function. *Plant Physiology, 117*, 337-43.

Heredia-Guerrero, J. A., San-Miguel, M. A., Sansom, M. S. P., Heredia, A., & Benítez, J. J. (2010). Aleuritic (9, 10, 16-trihydroxypalmitic) acid self-assembly on mica. *Physical Chemistry Chemical Physics, 12*, 10423-10428.

Jiménez-Bermúdez, S., Redondo-Nevado, J., Muñoz-Blanco, J., Caballero, J. L.,

886 López-Aranda, J. M., Valpuesta, V., Pliego-Alfaro, F., Quesada, M. A., &
887 Mercado, J. A. (2002). Manipulation of strawberry fruit softening by antisense
888 expression of a pectate lyase gene. *Plant Physiology, 128*, 751-759.
889 Kacuráková, M., Capek, P., Sasinková, V., Wellner, N., & Ebringerová, A. (2000).
890 FT-IR study of plant cell wall model compounds: Pectic polysaccharides and
891 hemicelluloses. *Carbohydrate Polymers, 43*, 195-203.
892 Kirby, A. R., Gunning, A. P., & Morris, V. J. (1996). Imaging polysaccharides by
893 atomic force microscopy. *Biopolymers, 38*, 355–366.
894 Kirby, A. R., MacDougall, A. J., & Morris, V. J. (2008). Atomic force microscopy
895 of tomato and sugar beet pectin molecules. *Carbohydrate Polymers, 71*, 640-
896 647.
897 Largo-Gosens, A., Hernández-Altamirano, M., García-Calvo, L., Alonso-Simón,
898 A., Álvarez, J., & Acebes, J.L. (2014). Fourier transform mid infrared
899 spectroscopy applications for monitoring the structural plasticity of plant cell
900 walls. *Frontiers in Plant Science*, *5*, 303. doi: 10.3389/fpls.2014.00303
901 Liu, H., Chen, F., Yang, H., Yao, Y., Gong, X., Xin, Y., & Ding, C. (2009). Effect
902 of calcium treatment on nanostructure of chelate-soluble pectin and
903 physicochemical and textural properties of apricot fruits. *Food Research*
904 *International, 42*, 1131-1140.
905 Manrique, G. D., & Lajolo, F. M. (2002). FT-IR spectroscopy as a tool for
906 measuring degree of methyl esterification in pectins isolated from ripening
907 papaya fruit. *Postharvest Biology and Technology, 25*, 99-107.
908 Marín-Rodríguez, M. C., Orchard, J., & Seymour, G. B. (2002). Pectate lyase, cell
909 wall degradation and fruit softening. *Journal of Experimental Botany, 53*,
910 2115–2119.
911 Marry, M., Roberts, K., Jopson, S. J., Huxham, M., Jarvis, M. C., Corsar, J.,
912 Robertson, E., & McCann, M. C. (2006). Cell-cell adhesion in fresh sugar-beet
913 root parenchyma requires both pectin esters and calcium cross-links.
914 *Physiologia Plantarum, 126*, 243-256.
915 Medina-Escobar, N., Cárdenas, J., Moyano, E., Caballero, J. L., & Muñoz-Blanco,
916 J. (1997). Cloning, molecular characterization and expression pattern of a
917 strawberry ripening-specific cDNA with sequence homology to pectate lyase
918 from higher plants. *Plant Molecular Biology, 34*, 867-877.

Mercado, J. A., Pliego-Alfaro, F., & Quesada, M. A. (2011). Fruit shelf life and potential for its genetic improvement. In M. A. Jenks, & P. J. Bebeli (Eds.), *Breeding for Fruit Quality* (pp. 81-104). Oxford: John Wiley & Sons, Inc..

Moing, A., Renaud, C., Gaudillère, M., Raymond, P., Roudeillac, P., & Denoyes-Rothan, B. (2001). Biochemical changes during fruit development of four strawberry cultivars. *Journal of the American Society for Horticultural Science, 126*, 394-403.

Morris, V. J., Gromer, A., & Kirby, A. R. (2009). Architecture of intracellular networks in plant matrices. *Structural Chemistry, 20*, 255-261.

Morris, V. J., Kirby, A. R., & Gunning, A. P. (2010). *Atomic force microscopy for biologists*. London: Imperial College Press.

O'Neill, M. A., Ishii, T., Albersheim, P., & Darvill, A. G. (2004). Rhamnogalacturonan II: structure and function of a borate cross-linked cell wall pectic polysaccharide. *Annual Review of Plant Biology, 55*, 109-139.

Paniagua, C., Posé, S., Morris, V. J., Kirby, A. R., Quesada, M. A., & Mercado, J. A. (2014). Fruit softening and pectin disassembly: an overview of nanostructural pectin modifications assessed by atomic force microscopy. *Annals of Botany, 114*, 1375-1383.

Posé, S., García-Gago, J. A., Santiago-Doménech, N., Pliego-Alfaro, F., Quesada, M. A., & Mercado, J. A. (2011). Strawberry fruit softening: role of cell wall disassembly and its manipulation in transgenic plants. *Genes, Genomes and Genomics, 5*, 40-48.

Posé, S., Kirby, A. R., Mercado, J. A., Morris, V. J., & Quesada, M. A. (2012). Structural characterization of cell wall pectin fractions in ripe strawberry fruits using AFM. *Carbohydrate Polymers, 88*, 882-890.

Posé, S., Paniagua, C., Cifuentes, M., Blanco-Portales, R., Quesada, M. A., & Mercado, J. A. (2013). Insights into the effects of polygalacturonase *FaPG1* gene silencing on pectin matrix disassembly, enhanced tissue integrity, and firmness in ripe strawberry fruits. *Journal of Experimental Botany, 64*, 3803-3815.

Quesada, M. A., Blanco-Portales, R., Posé, S., García-Gago, J. A., Jiménez-Bermúdez, S., Muñoz-Serrano, A., Caballero, J. L., Pliego-Alfaro, F., Mercado, J. A., & Muñoz-Blanco, J. (2009). Antisense down-regulation of the

952 *FaPG1* gene reveals an unexpected central role for polygalacturonase in
953 strawberry fruit softening. *Plant Physiology, 150*, 1022-1032.
954 Redgwell, R. J., Melton, L. D., & Brasch, D. J. (1992). Cell-wall dissolution in
955 ripening kiwifruit (*Actinidia deliciosa*). Solubilisation of the pectic polymers.
956 *Plant Physiology, 98*, 71-81.
957 Round, A. N., MacDougall, A. J., Ring, S. G., & Morris, V. J. (1997). Unexpected
958 branching in pectin observed by atomic force microscopy. *Carbohydrate*
959 *Research, 303*, 251-253.
960 Round, A. N., Rigby, N. M., MacDougall, A. J., Ring, S. G., & Morris, V. J.
961 (2001). Investigating the nature of branching in pectin by atomic force
962 microscopy and carbohydrate analysis. *Carbohydrate Research, 331*, 337-342.
963 Round, A. N., Rigby, N. M.., MacDougall, A. J., & Morris, V. J. (2010). A new
964 view of pectin structure revealed by acid hydrolysis and atomic force
965 microscopy. *Carbohydrate Research, 345*, 487-497.
966 Santiago-Doménech, N., Jiménez-Bermúdez, S., Matas, A. J., Rose, J. K. C.,
967 Muñoz-Blanco, J., Mercado, J. A., & Quesada, M. A. (2008). Antisense
968 inhibition of a pectate lyase gene supports a role for pectin depolymerization in
969 strawberry fruit softening. *Journal of Experimental Botany, 59*, 2769-2779.
970 Selvendran, R. R. (1985). Developments in the chemistry and biochemistry of
971 pectic and hemicellulosic polymers. *Journal of Cell Science, Supplement 2*, 51-
972 88.
973 Séné, C. F. B., McCann, M. C., Wilson, R. H., & Grinter, R. (1994). Fourier-
974 transform Raman and Fourier-transform infrared spectroscopy (an
975 investigation of five higher plant cell walls and their components). *Plant*
976 *Physiology, 106*, 1623-1631.
977 Sénéchal, F., Wattier, C., Rustérucci, C., & Pelloux, J. (2014).
978 Homogalacturonan-modifying enzymes: structure, expression, and roles in
979 plants. *Journal of Experimental Botany* DOI:10.1093/jxb/eru272
980 Sheehy, R. E., Kramer, M. K., & Hiatt, W. R. (1988). Reduction of
981 polygalacturonase activity in tomato fruit by antisense RNA. *Proceedings of*
982 *the National Academy of Sciences USA, 85*, 8805-8809.

983 Smith, C. J. S., Watson, C. F., Ray, J., Bird, C. R., Morris, P. C., Schuch, W., &
984 Grierson, D. (1988). Antisense RNA inhibition of polygalacturonase gene
985 expression in transgenic tomatoes. *Nature, 334*, 724-726.
986 Thibault, J.-F., Renard, C. M. G. C., Axelos, M. A. V., Roger, P., & Crépeau, M.-J.
987 (1993). Studies of the length of homogalacturonic regions in pectins by acid
988 hydrolysis. *Carbohydrate Research, 238*, 271-286.
989 Vicente, A. R., Saladié, M., Rose, J. K. C., & Labavitch, J. M. (2007). The linkage
990 between cell wall metabolism and fruit softening: looking to the future. *Journal*
991 *of the Science of Food and Agriculture, 87*, 1435–1448.
992 Villarreal, N. M., Rosli, H. G., Martínez, G. A., & Civello, P. M. (2008).
993 Polygalacturonase activity and expression of related genes during ripening of
994 strawberry cultivars with contrasting fruit firmness. *Postharvest Biology and*
995 *Technology, 47*, 141-150.
996 Walkinshaw, M. D., & Arnott, S. (1981). Conformations and interactions of
997 pectins. I. X-ray diffraction analyses of sodium pectate in neutral and acidified
998 forms. *Journal of Molecular Biology, 153*, 1055-1074.
999 Wang, H., Chen, F., Yang, H., Chen, Y., Zhang, L., & An, H. (2012). Effects of
1000 ripening stage and cultivar on physicochemical properties and pectin
1001 nanostructure of jujubes. *Carbohydrate Polymers, 89*, 1180-1188.
1002 Yang, H., An, H., Feng, G., Li, Y., & Lai, S. (2005). Atomic force microscopy of
1003 the water-soluble pectin of peaches during storage. *European Food Research*
1004 *and Technology, 220*, 587-591.
1005 Yang, H., Chen, F., An, H., & Lai, S. (2009). Comparative studies on
1006 nanostructures of three kinds of pectins in two peach cultivars using atomic
1007 force microscopy. *Postharvest Biology and Technology, 51*, 391-398.
1008 Yapo, B. M., Lerouge, P., Thibault, J.-F., & Ralet, M.-C. (2007). Pectins from
1009 citrus peel cell walls contain homogalacturonans homogeneous with respect to
1010 molar mass, rhamnogalacturonan I and rhamnogalacturonan II. *Carbohydrate*
1011 *Polymers, 69*, 426-435.
1012 Yapo, B. M. (2011). Pectic substances: from simple pectic polysaccharides to
1013 complex pectins - A new hypothetical model. *Carbohydrate Polymers, 86*, 373-
1014 385.
1015 Youssef, S. M., Jiménez-Bermúdez, S., Bellido, M. L., Martín-Pizarro, C.,

Barceló, M., Abdal-Aziz, S. A., Caballero, J. L., López-Aranda, J. M., Pliego-Alfaro, F., Muñoz, J., Quesada, M. A., & Mercado, J. A. (2009). Fruit yield and quality of strawberry plants transformed with a fruit specific strawberry pectate lyase gene. *Scientia Horticulturae, 119*, 120-125.

Youssef, S. M., Amaya, I., López-Aranda, J. M., Sesmero, R., Valpuesta, V., Casadoro, G., Blanco-Portales, R., Pliego-Alfaro, F., Quesada, & M. A., Mercado, J, A. (2013). Effect of simultaneous down-regulation of pectate lyase and endo-*β*-1,4-glucanase genes on strawberry fruit softening. *Molecular Breeding, 31*, 313-322.

Zdunek, A., Koziol, A., Pieczywek, P.M,, & Cybulska, J. (2014). Evaluation of the nanostructure of pectin, hemicellulose and cellulose in the cell walls of pears of different texture and firmness. *Food and Bioprocess Technology, 7*, 3525-3535.

Figures

Figure 1. ATR-FTIR spectra of CDTA (A) and sodium carbonate-soluble (B) pectin fractions in the 2000-800 cm^{-1} region. Pectins were extracted from ripe fruits of Control, *FaplC* (APEL) and *FaPG1* (APG) antisense transgenic lines (dashed, grey and black lines respectively). Inlet in Fig. 1-B shows detailed peaks of esterified (~1737 cm^{-1}) and desterified (~1625 cm^{-1}) carboxyl groups, displaying both transgenic lines a recalcitrant pool of esterified residues.

Figure 2. ~~Molecular mass~~ Chromatographic elution profiles of polyuronides extractable by CDTA (A, B) and sodium carbonate (C, D) from cell walls of wild-type, antisense *FaplC* (APEL; figures A,C) and antisense *FaPG1* (APG; figures B,D) ripe fruits. Profiles were obtained by ~~gel filtration~~ size exclusion chromatography on Sepharose CL-2B. Columns were calibrated by dextran blue and acetone for void volume (V_0) and total volume (V_T), respectively. Fractions were assayed for uronic acid and expressed as relative optical density (OD) at 515 nm. The results show the average profile of at least two independent chromatographic assays per sample.

~~**Figure 3.** (A) Representative image of CDTA pectins from strawberry ripe fruit obtained by AFM in contact mode. Branched pectin chains and micellar aggregates with emerging strands can be observed in the image. (B) Height profiles, showing the heights in a true branch point (black arrow) of a polymer chain (profile 1) and micellar aggregates (profile 2) with emerging strands of same height than isolated chains (grey arrow) and higher height at the core area (arrowhead).~~

Figure 3. Typical AFM images, in topographical mode, of ~~CDTA~~CSP-pectin samples from cell walls of wild-type (A), antisense *FaplC* (B) and antisense *FaPG1* (C) ripe fruits. Images 1-6 correspond to zoomed areas to show unbranched isolated chains (1,3), branched isolated molecules (5) and micellar aggregates (2,4,6). Scan size: 1 µm (A-C) and 250 nm (1-6).

Figure 4. Typical AFM images of ~~carbonate~~SSP-pectin samples from cell walls of

wild-type (A), antisense *FaplC* (B) and antisense *FaPG1* (C) ripe fruits. Images 1-6 correspond to zoomed areas to show unbranched isolated chains (1), branched molecules (3,4,5) and micellar aggregates (2,6). Scan size: 1 μm (A-C) and 250 nm (1-6).

Figure 5. Contour length distribution of CDTA (CSP) and sodium carbonate (SSP) soluble polymers isolated from fruit cell walls of control (A, E), antisense *FaplC* (APEL; figures B, F) and antisense *FaPG1* (APG; figures C, G) ripe fruits. Bars represent relative frequencies of the observed data ~~whilst the curved lines represent Log normal approximations~~. (D, H) Cumulative frequencies for CSP (D) and SSP (H) fractions, normalized to the maximum frequency value.

Figure 6. Average number of micellar aggregates in CDTA (CSP) and sodium carbonate (SSP) soluble pectin samples isolated from cell walls of control, antisense *FaplC* (APEL) and antisense *FaPG1* (APG) ripe fruits. For each pectin sample, bars with different letters indicate significant differences by Tukey test at P=0.05.

Figure 7. Schematic representation of a hypothetical mode of action for pectate lyase and polygalacturonase on CDTA and sodium carbonate pectin chains during strawberry ripening based on AFM analysis of antisense *FaplC* (APEL) and *FaPG1* (APG) ripe fruits. Length of pectin chains and branches, as well as the number of branches per chain are drawing at scale. Scissors indicate putative points of cutting for both enzymes. Pectate lyase would reduce HGA backbone length and the number of chain branches. This enzyme might play a minor role in the degradation of middle lamella pectins extracted with CDTA. Polygalacturonase has a more pronounced activity during strawberry ripening, degrading HGA backbone, and reducing the number of side-chains of pectins from both polyuronide fractions, as well as the length of sodium carbonate pectin side-chains.

Supplementary data

Supplementary Fig. S1. Aspect of plants and fruits from control and antisense *FaplC* (Apel39) and antisense *FaPG1* (APG29) genotypes.

Supplementary Fig. S2. (A) Representative image of CDTA pectins from strawberry ripe fruit obtained by AFM in contact mode. Branched pectin chains and micellar aggregates with emerging strands can be observed in the image. (B) Height profiles, showing the heights in a true branch point (black arrow) of a polymer chain (profile 1) and micellar aggregates (profile 2) with emerging strands of same height than isolated chains (grey arrow) and higher height at the core area (arrowhead).

The nanostructural characterization of strawberry pectins in pectate lyase or polygalacturonase silenced fruits elucidates their role in softening

Sara Posé[a1], Andrew R. Kirby[b], Candelas Paniagua[a], Keith W. Waldron[b], Victor J. Morris[b], Miguel A. Quesada[c], José A. Mercado[a]

[a]Instituto de Hortofruticultura Subtropical y Mediterránea "La Mayora" (IHSM-UMA-CSIC), Departamento de Biología Vegetal, Universidad de Málaga, 29071, Málaga, Spain

[b]Institute of Food Research, Norwich Research Park, Colney, Norwich, NR4 7UA, UK

[c]Departamento de Biología Vegetal, Universidad de Málaga, 29071, Málaga, Spain

e-mail: mercado@uma.es

Supplementary Fig. S1. Aspect of plants and fruits from control and antisense *FaplC* (Apel39) and antisense *FaPG1* (APG29) genotypes.

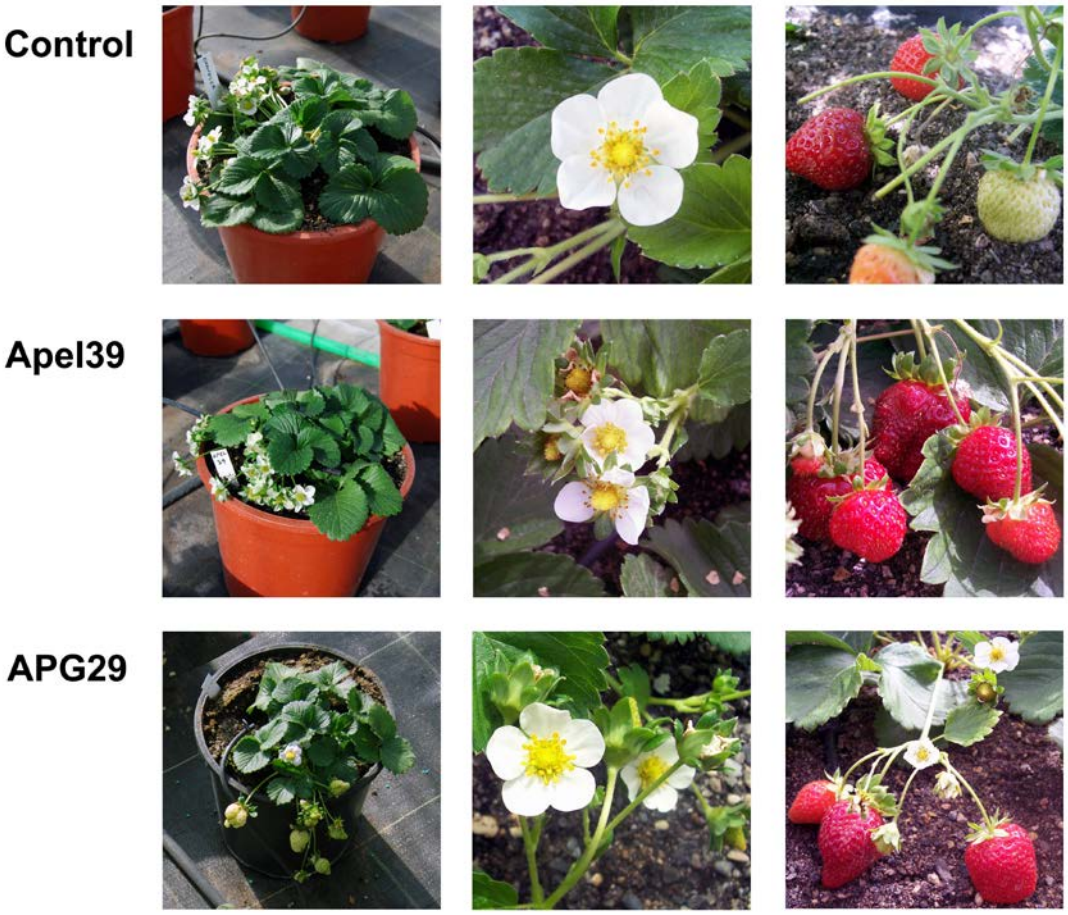

Supplementary Fig. S2. (A) Representative image of CDTA pectins from strawberry ripe fruit obtained by AFM in contact mode. Branched pectin chains and micellar aggregates with emerging strands can be observed in the image. (B) Height profiles, showing the heights in a true branch point (black arrow) of a polymer chain (profile 1) and micellar aggregates (profile 2) with emerging strands of same height than isolated chains (grey arrow) and higher height at the core area (arrowhead).